The Journal of Neuroscience, January 1995, 15(1): 865–874

Localization of GAT-1 GABA Transporter mRNA in Rat Striatum: Cellular Coexpression with GAD_{67} mRNA, GAD_{67} Immunoreactivity, and Parvalbumin mRNA

Sarah J. Augood,[1] Allan E. Herbison,[2] and Piers C. Emson[1]

[1]MRC Molecular Neuroscience Group, [2]Laboratory of Neuroendocrinology, Department of Neurobiology, The Babraham Institute, Babraham, Cambridge CB2 4AT, UK

The cellular localization and neurochemical phenotype of cells expressing the GAT-1 GABA transporter was investigated in the adult rat dorsal striatum using single and dual *in situ* hybridization and immunocytochemical techniques. Cellular sites of GAT-1, GAD_{67}, and parvalbumin mRNAs were visualized using a combination of radioactive and alkaline phosphatase-labeled oligonucleotides and emulsion autoradiography; GAD_{67} immunoreactivity was detected using a polyclonal antibody (K2) and 3′3″-diaminobenzidine. Two types of GAT-1–positive striatal cells were detected: (1) those expressing an abundance of GAT-1 mRNA, and (2) those expressing low/undetectable amounts of message. This study focused on the striatal cells expressing an abundance of GAT-1 mRNA; these cells accounted for approximately 3–5% of all striatal neurons and were detected scattered sparsely throughout the striatal complex. Dual *in situ* hybridization and immunocytochemical studies established that all cells enriched in GAT-1 mRNA also expressed high levels of GAD_{67} mRNA and were strongly GAD_{67} immunopositive; the converse was also found to be the case, the two hybridization signals having identical distribution patterns. Further dual *in situ* hybridization studies established that approximately 60% of these high GAD_{67}/GAT-1 cells expressed parvalbumin mRNA, a marker of one population of striatal interneurons, and had an average cross-sectional area of 152.40 μm^2. The chemical phenotype of the remaining 40% of high GAD_{67}/GAT-1 cells was not determined, although the average cross-sectional area of these cells (102.48 μm^2) was significantly smaller than GAT-1/GAD_{67}/parvalbumin cells; these cells were detected in all striatal regions and are likely to correspond to another population of striatal GABAergic interneuron.

[Key words: striatum, interneuron,* in situ *hybridization, GABA uptake, parvalbumin, GAD]

Immunocytochemical and molecular biological studies have established that glutamic acid decarboxylase (GAD), the enzyme involved in γ-aminobutyric acid (GABA) biosynthesis, exists as two isoforms termed GAD_{65} and GAD_{67}, which differ in their size, cofactor association, subcellular distribution (Erlander et al., 1991; Kaufman et al., 1991), and display similar but distinct patterns of expression within the rat striatum (Erlander et al., 1991; Mercugliano et al., 1992; Esclapez et al., 1993, 1994). The majority of striatal cells, medium-sized spiny efferents, express an abundance of GAD_{65} mRNA while the small population of local circuit GABAergic interneurons are preferentially enriched in GAD_{67} mRNA (Mercugliano et al., 1992). Indeed, a similar heterogeneous distribution of GAD mRNA is detected in postmortem monkey and human tissue (Herrero et al., 1993). Immunocytochemical studies using anti-GAD antibodies in colchicine-treated rats report that two populations of cells are detected (1) those that display weak GAD immunoreactivity, are medium sized (10–15 μm in diameter) and account for approximately 30–85% of striatal cells, and (2) those that are intensely stained for GAD and account for 3–20% of striatal neurons (Bolam et al., 1985; Kita and Kitai, 1988; Kubota et al., 1987). Ultrastructural examination of these strongly stained GAD cells show that they all display nuclear indentations and range in size from small- to medium-sized to large with somatic areas of 90 μm^2 and 200 μm^2, respectively (Bolam et al., 1985; Kita and Kitai, 1988; Kubota et al., 1987). The somatic morphology of these strongly GAD-immunoreactive cells is consistent with them being local circuit interneurons, although neither cell type was immunoreactive for somatostatin or choline acetyl-transferase (Kita and Kitai, 1988)—chemical markers of two populations of striatal interneurons. Further, a scattering of densely labeled GAD_{67} mRNA striatal cells has been reported (Chesselet and Robbins, 1989; Mercugliano et al., 1992; Esclapez et al., 1993, 1994) that are likely to correspond to this small population of strong GAD-immunoreactive cells. In agreement with the immunocytochemical studies, these high GAD_{67} mRNA cells do not express NADPH-diaphorase activity (Chesselet and Robbins, 1989), a marker of striatal somatostatin interneurons (Vincent and Johansson, 1983). More recent immunocytochemical studies have shown that some strongly immunoreactive GABA cells are also immunoreactive for parvalbumin (PV: Cowan et al., 1990; Kita et al., 1990); a calcium-binding protein associated with fast-twitch skeletal muscles (Schwartz and Kay, 1988) and fast-spiking neurons in rat (Celio 1986; Kawaguchi et al., 1987; Kawaguchi and Kubota, 1993) and avian brain (Braun et al., 1985). While the precise functional role(s) of this calcium-binding protein are still unknown, it has been suggested that PV may be involved in the reduction of intracellular calcium concentrations following depolarization. Indeed, the in-

May 2, 1994; revised July 18, 1994; accepted July 20, 1994.

We thank Dr. J. Bicknell for his constructive critique of this manuscript, Mrs. K. Westmore for excellent technical assistance, and Mr. I. King for emulsion autoradiography. The MRC is thanked for financial support. S.J.A. is a Wellcome Trust Mental Health Research Fellow. A.E.H. is a Lister Institute-Jenner Fellow.

Correspondence should be addressed to Sarah J. Augood at the above address.

tracellular concentration of PV in several groups of CNS neurons has been estimated to be in the micromolar range, a concentration consistent with a calcium-buffering role of this protein within these neurons (Plogman and Celio, 1993).

The reuptake of GABA into presynaptic nerve terminals is believed to be the principle mechanism for terminating GABA neurotransmission; the activity of this uptake process may be an index of presynaptic GABA activity. Thus, to examine if striatal cells enriched in GAD protein (Cowan et al., 1990; Kita et al., 1990) and GAD_{67} mRNA (Mercugliano et al., 1992; Esclapez et al., 1993, 1994) were also enriched in GAT-1 mRNA, a member of the neuronal GABA transporter family, dual *in situ* hybridization studies were carried out on striatal tissue from mature adult rats. Further, immunocytochemical and *in situ* hybridization techniques were combined to visualize, simultaneously on the same tissue section, cells enriched in GAD_{67} immunoreactivity and cells enriched in GAT-1 gene transcripts. The expression of PV mRNA was included in the study (1) as a chemical marker of a subpopulation of GABAergic aspiny local circuit neurons, and (2) to determine unambiguously if cells expressing both GAD_{67} and PV were enriched in the GAT-1 GABA transporter gene.

Materials and Methods

Animals. Adult Wistar rats, bred from the Babraham colony, had free access to food and water at all times. For all the *in situ* hybridization studies, fresh frozen cryostat sections were cut (10 μm), collected directly onto RNase-free gelatinized slides, and stored at −80°C until processed. For the dual immunocytochemical and *in situ* hybridization studies, three rats were anaesthetized with Avertin and perfused through the heart with heparinized saline (10,000 IU heparin/ml) followed by a Tris-buffered saline (TBS), 4% paraformaldehyde solution. The brains were removed and placed overnight in a 25% sucrose-TBS solution made using autoclaved water and containing 1000 U/liter RNA guard (Pharmacia, Milton Keynes, UK). Brains were then sectioned (25 μm) in the coronal plane on a sliding microtome and collected into TBS containing RNA guard.

Oligonucleotides. Antisense oligonucleotides complementary to nucleotides 489–517 of the rat GAD_{67} gene (Julien et al., 1990), nucleotides 153–185 of the rat GAT-1 GABA transporter gene (Guastella et al., 1990), and nucleotides 140–184 of the rat PV gene (Epstein et al., 1986) were synthesized using an automated DNA synthesizer and purified by gel filtration. The antisense GAD_{67} oligonucleotide was labeled directly with alkaline phosphatase (AP) according to the method of Jablonski and colleagues (1986) and purchased from Syngene Inc., San Diego. The PV and GAT-1 antisense oligonucleotides (100 ng) were 3′ end-labeled with α^{35}S-dATP using calf intestinal terminal deoxynucleotidyl transferase (48 U; Pharmacia, Milton Keynes, UK) to a specific activity of $>1 \times 10^7$ dpm/μg and stored at −20°C until used. The specificity of the PV and GAD_{67} oligonucleotide sequences for detecting PV and GAD_{67} gene transcripts, respectively, in rat brain has been demonstrated previously (Seto-Ohshima et al., 1989; Herbison et al., 1992).

Northern analysis. Total RNA was isolated from fresh frozen rat cerebellar tissue using the method of Chomczynski and Sacchi (1987), size separated on a 1% agarose/MOPS gel, capillary blotted onto a nylon membrane (Hybond-N; Amersham Int.,) with 10× SSC, and incubated in prehybridization buffer for 3 hr at 40°C as described previously (Augood and Emson, 1994). The antisense GAT-1 oligonucleotide (100 ng) was 3′ end-labeled with α^{32}P-dATP using terminal deoxynucleotidyl transferase (48 U), purified on a Sephadex G-50 column, and added directly to the prehybridization buffer. Following an overnight hybridization at 40°C, the membrane was washed stringently (1× SSC/0.1% SDS for 15 min at 40°C then 30 min at 50°C) and exposed to Hyperfilm-MP (Amersham Int., Amersham, UK) with intensifying screens for 5.5 d at −80°C, then developed using an automated film processor (Fuji RG II).

In situ *hybridization.* Tissue sections were taken directly from the −80°C freezer, warmed to room temperature, fixed (15 min) in 4% neutral-buffered paraformaldehyde/0.1 M phosphate buffer, rinsed briefly with 0.1 M phosphate-buffered saline, and dehydrated through a series of graded alcohols. Labeled oligonucleotides were diluted in hybridization buffer containing 50% deionized formamide, 10% dextran sulphate, 1× Denhardts solution, 4× SSC, 250 μg/ml denatured salmon testis DNA, and 0.3% β-mercaptoethanol and 1–2 ng of diluted probe was applied to each slide containing three to four tissue sections.

For the dual *in situ* hybridization studies, the two oligonucleotides either AP-GAD_{67} and ^{35}S-GAT-1 (Experiment A) or AP-GAD_{67} and ^{35}S-PV (Experiment B) were diluted in the same hybridization buffer (containing 35% deionized formamide) and applied to the same tissue section. Following an overnight hybridization at 37°C, sections were washed in 1× SSC at 55°C (3 times 30 min) then either (1) dehydrated and processed for emulsion autoradiography (Ilford K5) for the radioactive probes alone, or (2) processed for AP color development to visualize cellular sites of GAD_{67} gene expression then emulsion autoradiography to visualize cellular sites of either PV or GAT-1 gene expression, as described previously (Augood et al., 1993; Augood and Emson, 1994).

For the dual *in situ* hybridization studies, where two oligonucleotides were applied simultaneously to the same tissue section, displacement experiments were carried out to demonstrate that the radioactive oligonucleotide hybridized specifically to the tissue section and was not sticking nonspecifically to the AP-GAD_{67} probe. For these experiments, a 50-fold excess of unlabeled PV or GAT-1 oligonucleotide (as appropriate) was added to the hybridization buffer containing the two labeled probes (either Experiment A, AP-GAD_{67} and ^{35}S-GAT-1, or Experiment B AP-GAD_{67} and ^{35}S-PV) and processed as described above. Further, to demonstrate that the ^{35}S-PV oligonucleotide hybridized to the same cells in the presence of the AP-GAD_{67} probe, additional sections were hybridized with the ^{35}S-PV probe alone (Experiment C) and the distribution and mean somatic area of striatal PV mRNA-containing cells compared with data from the dual *in situ* hybridization study (Experiment B).

Only sections hybridized with the ^{35}S-PV probe alone were counterstained, rapidly dehydrated, and coverslipped with Ralmount (BDH Laboratory Supplies, Lutterworth, Leics, UK); dual *in situ* hybridization sections were not counterstained but, instead, were coverslipped, hydrated, using glycerin jelly, and stored at 4°C in the dark.

Data analysis. The mean cross-sectional area of cells expressing either (A) GAT-1 and GAD_{67} mRNAs, (B) GAD_{67} and PV mRNAs, or (C) PV mRNA was measured using a computer-assisted image analysis system (Seescan Satellite, Cambridge, UK). Tissue sections were viewed under bright-field illumination (Leitz microscope) using a 40× objective, a neutral density filter (1.0), and a stabilized light source (set at 2.5). The software was calibrated under 40× magnification with a graticule (for 10 μm scale = 0.58) so that accurate area measurements could be made. Live on-line microscopic images were captured by a video camera (Sony XC/77CE), digitized, and displayed on the color monitor. Individual somatic area measurements were made by tracing round the outline of the cell cytoplasm with the aid of a cursor; the filled area covering the cell body would then be calculated in units of μm^2. This procedure was repeated for each cell measured.

For analysis of the AP-GAD_{67}/^{35}S-GAT-1 (Experiment A) coexpression studies, striatal sections (coronal) were divided into three areas, periventricular (P: adjacent to the lateral ventricle), midstriatum (M), and lateral striatum (L), as shown in Figure 6, and the cross-sectional area of cells within these three designated areas measured. Generally, sections were scanned in a standardized fashion; cells in the periventricular region would be measured first then individual cell measurements would be taken while the section was being transversed in the mediolateral direction.

An estimate of the percentage of neurons that express both GAD_{67} and GAT-1 gene transcripts in the rat dorsal striatum was made using computer-assisted image analysis. Tissue sections were viewed under bright-field illumination using a 10× objective and images capture by a video-camera as described above. The percentage of double-labeled neurons was estimated for each field by manually counting the number of positive neurons within the field and expressing this figure as a percentage of the total number of neurons visible. A total of nineteen separate fields were sampled from four rats.

Combined GAD immunocytochemistry and GAT-1 in situ *hybridization.* Immunostaining was carried out first by incubating free-floating coronal sections (25 μm) containing the dorsal striatum in a polyclonal antiserum directed against GAD_{67} (K2, 1:300; Chemicon Int.) for 40 hr at 4°C. This antibody was raised in rabbits against GAD_{67} protein de-

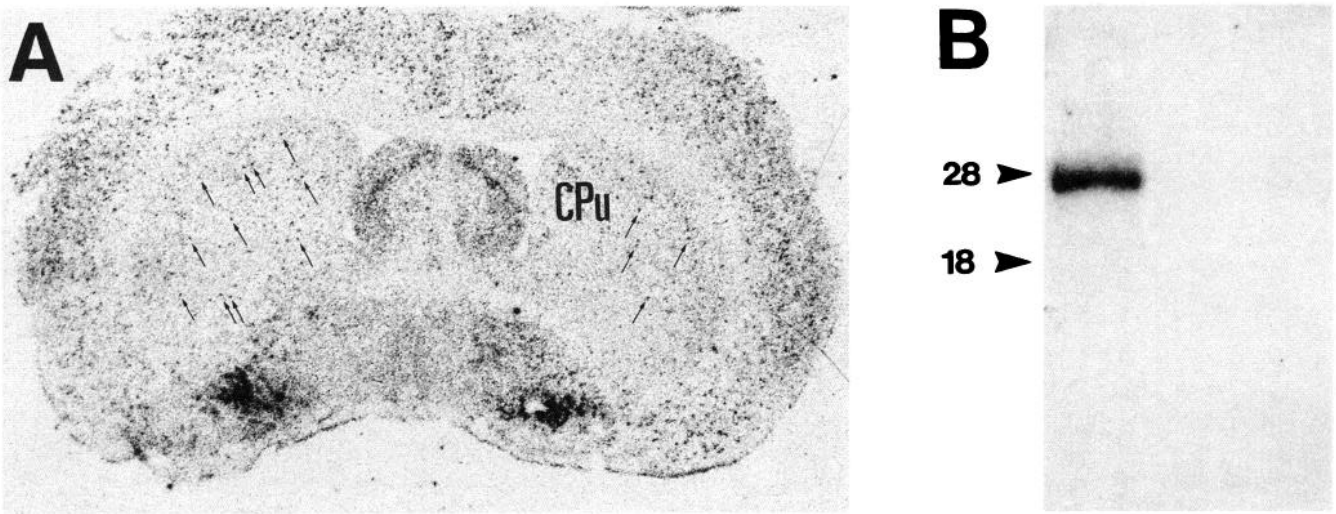

Figure 1. *A,* Direct autoradiographic print showing the distribution of GAT-1 mRNA in a coronal section of rat brain visualized using the ^{35}S-GAT-1 oligonucleotide and *in situ* hybridization. A strong hybridization signal is detected in the cerebral cortex, lateral septum, diagonal band of Broca, and in discrete cells scattered throughout the mediolateral striatal (*CPu*) axis (*arrows*). *B,* Northern analysis of total RNA isolated from rat cerebellar cortex and hybridized with the ^{32}P-GAT-1 oligonucleotide. A single band of approximately 4.5 kb is detected. Positions of 28S and 18S ribosomal RNA are marked.

rived from a bacterial expression system and has been characterized extensively elsewhere (Gonzales et al., 1991; Kaufman et al., 1991; Esclapez et al., 1994). The antiserum was diluted in double-distilled, autoclaved TBS containing 0.1% bovine serum albumin and RNA guard. Immunoreactivity was visualized using peroxidase-labeled goat anti-rabbit immunoglobulins (1:500; Vector Labs, UK) and hydrogen peroxidase-activated 3,3′-diaminobenzidine (DAB: 0.5 mg/ml). Sections were washed several times in TBS, then once rapidly in water before being mounted on gelatinized RNase-free slides. *In situ* hybridization using the ^{35}S-labeled GAT-1 oligonucleotide was then carried out as described above. Finally, sections were processed for emulsion autoradiography (6 weeks) then coverslipped without counterstaining.

Results

The regional distribution of GAT-1 mRNA in rat forebrain was observed, initially, on film autoradiograms. Figure 1*A* shows the distribution of GAT-1 gene transcripts in the caudal aspect of the rat dorsal striatum (CPu); individual cells enriched in GAT-1 mRNA are detected scattered throughout the dorsolateral axis (arrows). A strong GAT-1 hybridization signal is detected also in the cerebral cortex, diagonal band of Broca, and lateral septum. No hybridization signal was detected on film autoradiograms for tissue sections hybridized in the presence of an excess of unlabeled GAT-1 probe, demonstrating that the binding of this probe sequence to brain sections was displaceable. Further, Northern analysis of total RNA isolated from rat cerebellar tissue and hybridized with the ^{32}P-labeled GAT-1 oligonucleotide showed a single intense band of approximately 4.5 (kilobase) kb (Fig. 1*B*). The size of this single band is in good agreement with human nuclease protection assays (Xia et al., 1993) and rat RNA studies (Guastella et al., 1990; Gomeza et al., 1994), demonstrating further the specificity of this probe sequence.

The GAT-1 oligonucleotide used in this study shares only 52% and 58% nucleotide sequence homology with GAT-2 and GAT-3, respectively; other members of the GABA transporter gene family (Borden et al., 1992). Indeed, Clark and colleagues (1992) report that GAT-B (GAT-3) is not expressed in the striatum and is virtually undetectable in the cerebral cortex, suggesting that the GAT-1 oligonucleotide used in this study, which displays a strong hybridization signals in the cerebral cortex and in discrete cells in the striatum (see Figs. 1, 2*B,D*), is not cross-hybridizing to GAT-B mRNA *in vitro*.

For the single *in situ* hybridization studies, cellular sites of GAT-1 mRNA and PV mRNA were detected by the accumulation of silver grains overlying weak methylene blue-counterstained cell somata (Fig. 2).

Cellular sites of GAD_{67} mRNA were detected by the presence of a purple AP reaction product concentrated within the cytoplasm of cells; sections were not counterstained before being coverslipped. For the dual *in situ* hybridization studies, where two gene transcripts were expressed by the same cell, silver grain clusters were seen overlying cells containing an AP reaction product (see Figs. 3*B,D*; 4*C*). For the combined GAD immunocytochemistry and GAT-1 *in situ* hybridization study, silver grain clusters were detected overlying cells stained with the DAB chromogen (Fig. 5). On all control sections, hybridized in the presence of an excess of unlabeled probe, no silver grain clusters were detected overlying cell bodies, demonstrating that the binding of the radiolabeled PV/GAT-1 probes to the tissue sections was displaceable. Equally, silver grain clusters were abolished in the combined immunocytochemistry and *in situ* hybridization experiments by addition of an excess of GAT-1 unlabeled probe.

Experiment A: coexpression of GAD_{67} and GAT-1 mRNAs

For these dual *in situ* hybridization studies, the two gene transcripts were observed simultaneously on the same tissue section using bright-field microscopy. Cellular sites of GAD_{67} transcripts were visualized by the accumulation of AP reaction product in the cell cytoplasm while GAT-1 transcripts were visualized by the accumulation of silver grain clusters overlying cell bodies (Fig. 3*B,D*). In all dorsal striatal areas (P, M, and L), silver grain clusters (GAT-1 mRNA) were associated with strong AP positive (GAD_{67} mRNA) cell bodies, demonstrating clearly that the two gene transcripts were expressed in the same cell. Cells enriched in GAD_{67} and GAT-1 gene transcripts were seen scattered sparsely throughout the entire neostriatum (see Fig.

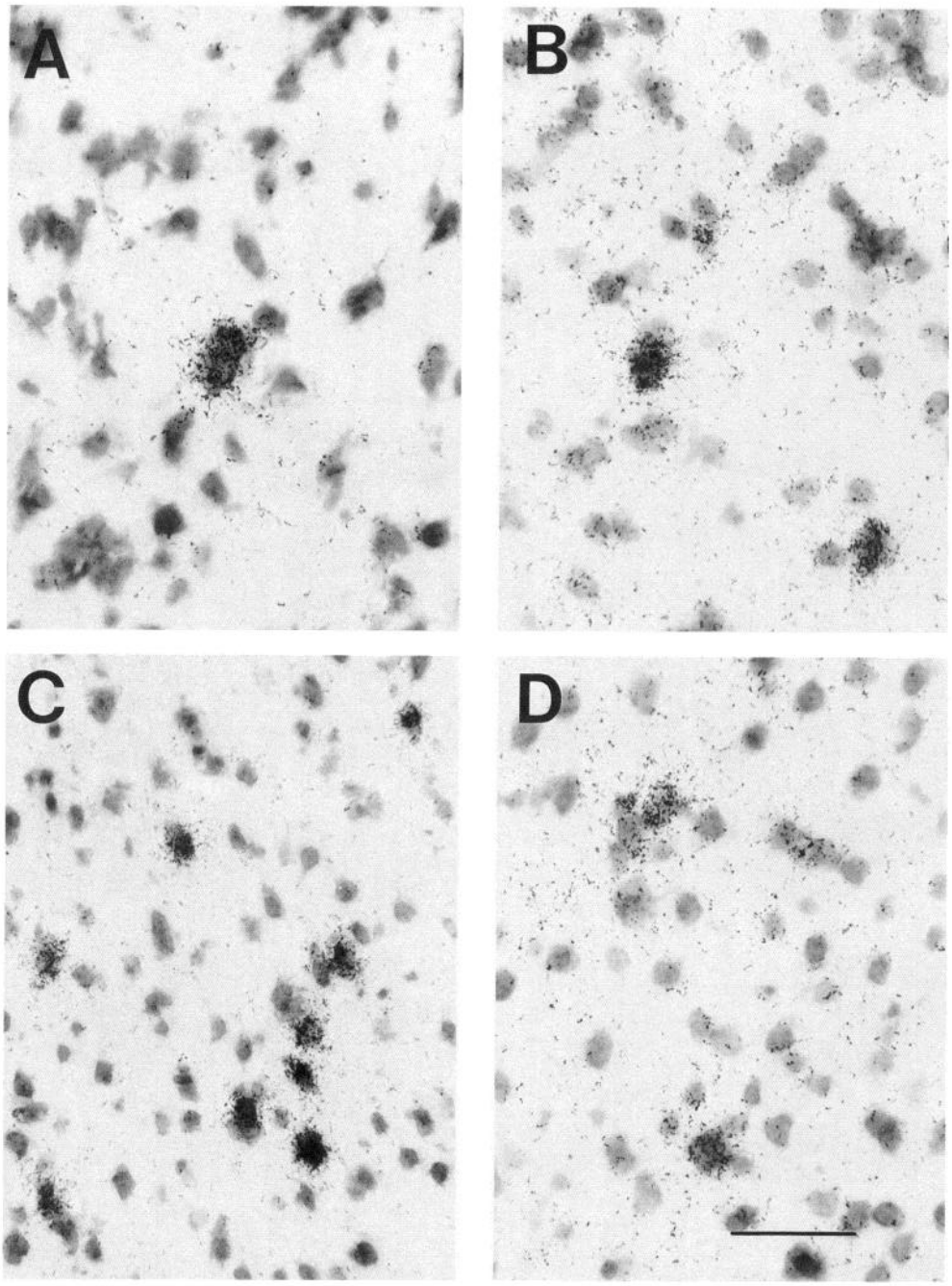

Figure 2. Cellular localization of PV mRNA and GAT-1 mRNA in the rat dorsal striatum (*A* and *B*) and frontal cortex (*C* and *D*). Sections have been hybridized with either the ^{35}S-PV oligonucleotide (*A* and *C*) or the ^{35}S-GAT-1 oligonucleotide alone and processed for emulsion autoradiography. Cellular sites of hybridization are detected by the accumulation of silver grains overlying weak methylene blue counterstained cell bodies. Scale bar = 50 μm.

3*A,C*). Using this dual *in situ* hybridization technique some background staining of tissue sections occurs, which acts as a light counterstain allowing the outline and spatial distribution of all perikarya to be visualized. The relative abundance of GAD_{67} mRNA or GAT-1 mRNA in the majority of striatal cells, presumably medium-sized spiny output cells, was low/undetectable (at this emulsion exposure time) when compared with the high GAD_{67}/GAT-1 expressing cells, which we estimate to account for approximately 4.4 ± 1.2% (219 positive cells out of a total of 5152 striatal neurons).

On coronal sections, the cross-sectional somatic area of individual high GAD_{67}/GAT-1 expressing cells was determined in the periventricular (P), mid (M), and lateral (L), as shown in Figure 6; the average cross-sectional areas of GAD_{67}/GAT-1 expressing cells in these three striatal regions are shown in Table 1. Figure 3 shows the scattered distribution of high GAD_{67}/GAT-1 expressing cells in the periventricular (P: Fig. 3*A*) and mid (M: Fig. 3*C*) striatal areas; at higher power periventricular GAD_{67}/GAT-1 cells (arrowed cells in Fig. 3*B*) are visibly smaller than midstriatal GAD_{67}/GAT-1 cells (arrowed cells in Fig. 3*D*).

Experiment B: coexpression of GAD_{67} and PV mRNAs

In contrast to Experiment A, not all AP-stained striatal cells (high GAD_{67} mRNA cells) were overlain with silver grains (PV mRNA). Two distinct populations of cells were observed, one labeled with both AP reaction product and silver grains (high GAD_{67}/PV cells; filled arrow cells in Fig. 4*C*) and the other labeled with AP reaction product alone (high GAD_{67} cells; see

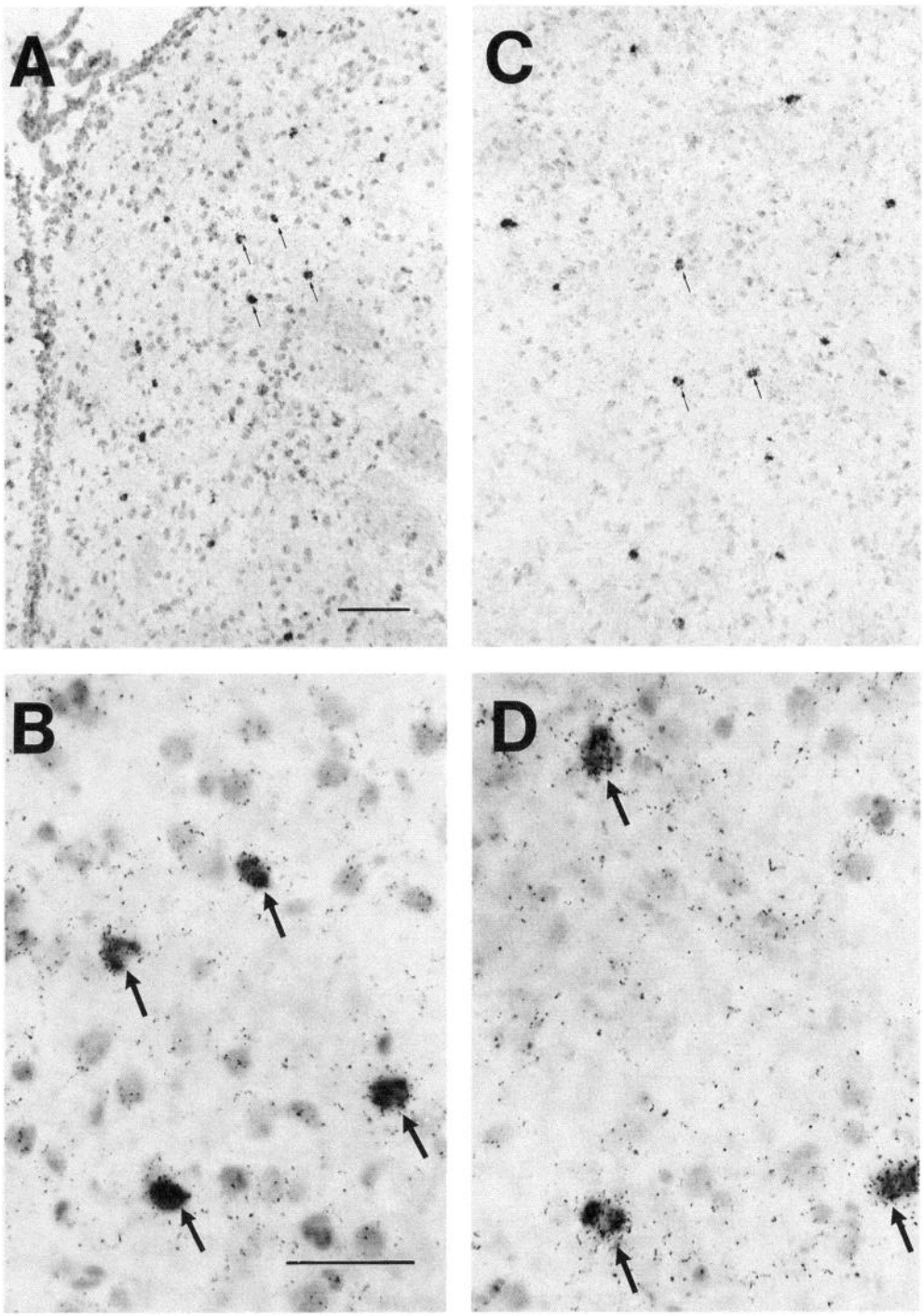

Figure 3. Cellular localization of GAD_{67} mRNA (AP probe) and GAT-1 mRNA (^{35}S probe) in a coronal section of rat dorsal striatum. Cellular sites of GAD_{67} mRNA are visualized by the accumulation of AP reaction product in the cytoplasm while cellular sites of GAT-1 mRNA are labeled with silver grain clusters. Cells expressing both gene transcripts are labeled with AP reaction product and overlain with silver grain clusters. GAD_{67} mRNA and GAT-1 mRNA are selectively enriched in the same cells in the periventricular (*arrows in A and B*) and mid (*arrows in C and D*) striatal regions. *B* and *D* are high power magnifications of *A* and *C*, respectively. Scale bars: *A* and *C* = 200 μm, *B* and *D* = 50 μm.

filled arrow cells Fig. 4*A,B,D*). The spatial distribution of these two cell populations was similar but not identical; non-PV high GAD_{67} mRNA-expressing cells were detected in all striatal regions, whereas the distribution of PV/GAD_{67} mRNA positive cells was more restricted; no cells were detected in the periventricular (P) area (see Fig. 6). The density and cross-sectional area of cells in the lateral (L) striatum was visibly greater than in any other striatal region. The average cross-sectional area of non-PV high GAD_{67} cells (filled arrow in Fig. 4*A,B,D*) was significantly smaller than high GAD_{67}/PV cells (filled arrows in Fig. 4*C*) measured on the same tissue sections (see Table 1). Occasionally cells were detected that were overlain with silver grains (PV mRNA) but not enriched in AP reaction product (GAD_{67} mRNA; open arrows in Fig. 4*C,D*); these PV-positive cells were rare and appeared to be smaller than high GAD_{67}/PV cells.

Experiment C: expression of PV mRNA

On tissue sections hybridized with the ^{35}S-PV probe alone, numerous PV positive cells (overlain with silver grains) were detected in the cerebral cortex (with the exception of layer I; Fig. 2*C*) and scattered sparsely throughout the entire striatal complex (Fig. 2*A*), with the exception of the periventricular region adjacent to the lateral ventricle. No ^{35}S-PV mRNA-containing

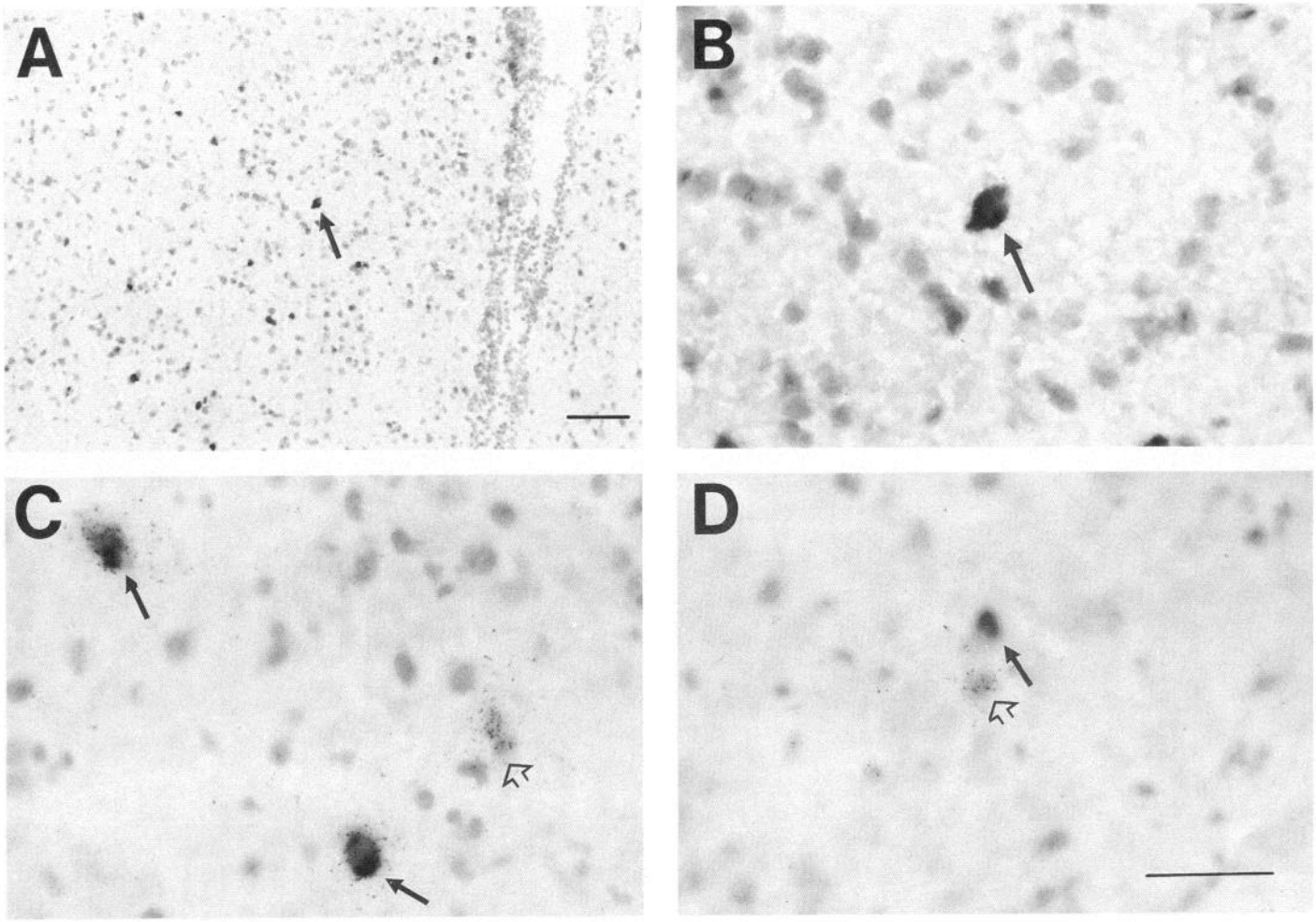

Figure 4. Coronal section of rat dorsal striatum hybridized simultaneously with the AP-GAD67 and ^{35}S-PV oligonucleotides. An example of the same high GAD_{67} expressing cell is illustrated (*arrow*) in *A* and *B*. This cell is not overlain with silver grains, demonstrating that it is a non-PV high GAD_{67} expressing cell. In contrast, on the same tissue section, numerous examples of cells enriched in both GAD_{67} mRNA and PV mRNA can be found (*filled arrows in C*), as can occasional cells that express PV mRNA (*silver grains*) alone and are not particularly enriched in GAD_{67} mRNA (*open arrows in C and D*). These cells are rare. Scale bars: *A* = 100 μm, *B, C,* and *D* = 50 μm.

cells were detected in this discrete striatal area (see Fig. 6). It was noted, however, that both the density and the cross-sectional somatic area of PV mRNA-positive cells was greater in lateral (L) than in medial (M) striatal regions, an observation consistent with the coexpression data presented above and with the immunocytochemical findings of others (Gerfen et al., 1985; Cowan et al., 1990; Kubota et al., 1993). From the total number of ^{35}S-PV mRNA-positive cells sampled by computer-assisted image analysis (n = 136), it was determined that the average cross-sectional area of this cell population on 10 μm thick cryostat sections was 163.14 ± 64.42 μm^2 (mean ± SD) with a range of 66–382 μm^2; these data are presented in Table 1.

Combined GAD immunocytochemistry and GAT-1 in situ *hybridization*

GAD_{67} immunoreactive structures were detected by the deposition of brown DAB reaction product concentrated within the cytoplasm of immunoreactive perikarya. In striatum, numerous GAD_{67}-immunoreactive cell bodies were seen scattered sparsely upon a background of light neuropil staining (Fig. 5*A,B*). GAD_{67}-immunoreactive cell processes were not observed and striatal fiber bundles were not stained. On the same tissue section, cellular sites of GAT-1 mRNA were detected by silver grain clusters overlying cell bodies; clusters were always detected overlying GAD_{67}-immunoreactive cells (Fig. 5*C,D*), demonstrating that cells enriched in GAD_{67} immunoreactivity were also enriched in GAT-1 mRNA. On control sections processed with an excess of unlabeled GAT-1 probe, silver grain clusters were not observed, demonstrating that the binding of the radiolabeled GAT-1 probe was displaceable and was not binding nonspecifically to the DAB reaction product.

Discussion

In this study we have mapped the distribution and characterized the chemical phenotype of cells enriched in GAT-1 mRNA in the rat dorsal striatum. We report, for the first time, that GAT-1 mRNA is particularly enriched in approximately 3–5% of striatal cells, which also express an abundance of GAD_{67} mRNA and GAD_{67} immunoreactivity, suggesting strongly that, in the dorsal striatum at least, expression of this gene is restricted to neurons and not glia. An appreciable GAT-1 mRNA hybridization signal has been reported, however, in Bergmann glia (Rattray and Priestley, 1994).

Striatal somata enriched in GAT-1 mRNA are sparsely dis-

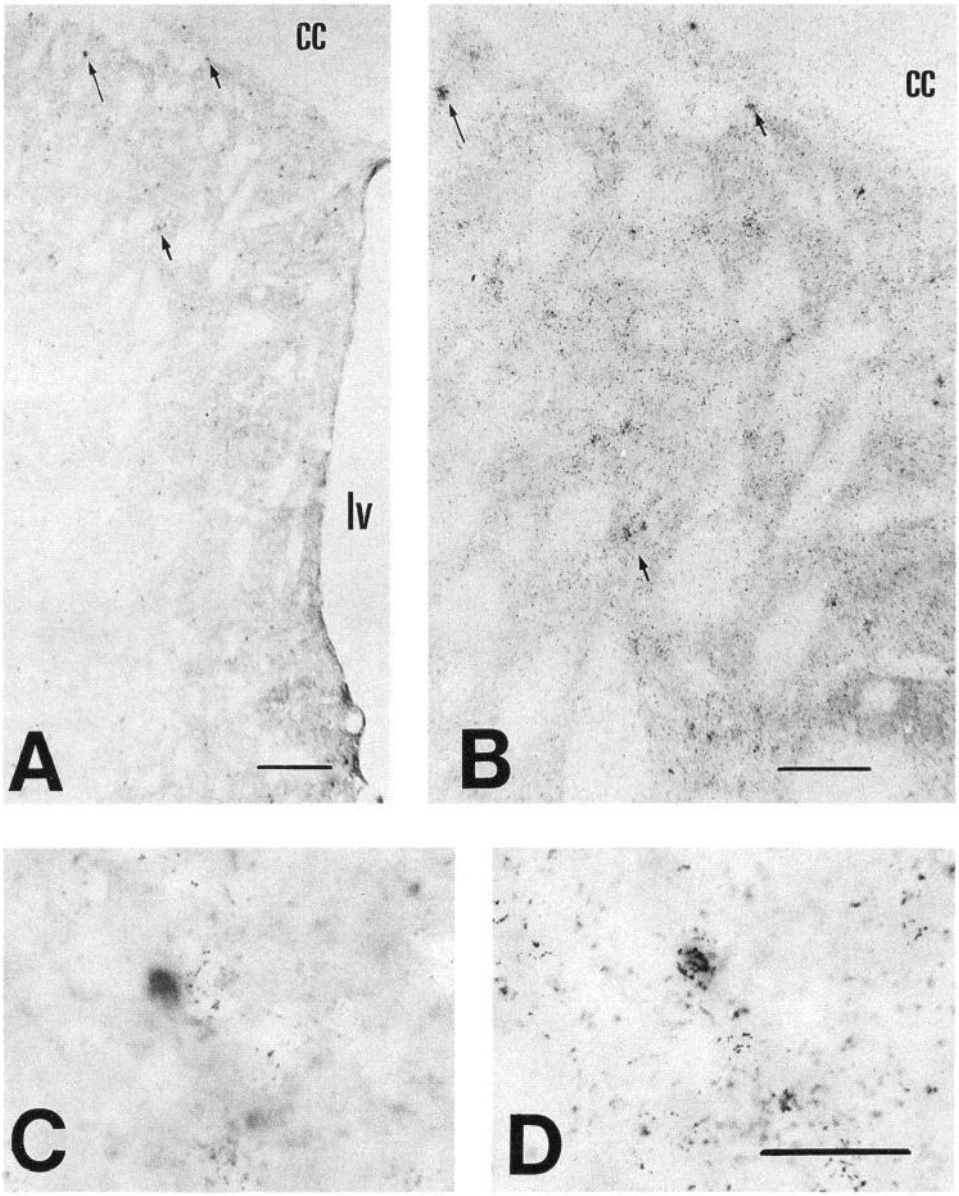

Figure 5. A coronal section of dorsal striatum processed for GAD immunocytochemistry and GAT-1 *in situ* hybridization. Isolated GAD_{67}-immunoreactive cell bodies are detected upon a background of light neuropil staining (*arrows in A and B*). Cellular sites of GAT-1 mRNA are detected by the accumulation of silver grains overlying cell somata. *C* and *D*, An individual striatal cell immunopositive for GAD_{67} protein (*in focus in C*) and expressing GAT-1 mRNA (*silver grains in D*). The DAB and silver grain clusters are in two different focal planes, allowing the simultaneous visualization of the two GABA markers in the same cell. Lateral ventricle (*lv*); corpus callosum (*cc*). Scale bars: *A* = 200 μm; *B* = 100 μm; *C* and *D* = 50 μm.

tributed throughout all areas of the neostriatal complex, although detected more frequently in lateral than in medial striatal regions and have a cross-sectional area from 40–345 μm^2 on 10 μm thick cryostat sections. Using both dual *in situ* hybridization (coexpression) and combined immunocytochemistry and *in situ* hybridization, we have shown that dorsal striatal cells enriched in GAT-1 mRNA are also enriched in GAD_{67} mRNA (Fig. 3) and GAD_{67} immunoreactivity (Fig. 5). The distribution of cells enriched in GAD_{67} mRNA reported herein is in good agreement with the studies of others (Chesselet and Robbins 1989; Esclapez et al., 1993, 1994; Mercugliano et al., 1992; Herrero et al., 1993). Taken together, these data suggest strongly that these GABA cells use the high-affinity GAT-1 GABA transporter protein for GABA reuptake. It is of interest to note that GABA transaminase activity, the enzyme responsible for the degradation of GABA, is also reported to be enriched in sparsely scattered medium-sized (13–21 μm diameter) striatal cells with triangular or fusiform somata and varicosed dendrites (Nagai et al., 1983); morphological features characteristic of GABAergic interneurons (Bolam et al., 1985). The spatial distribution of these GABA transaminase-enriched cells parallels the distribution of cells enriched in GAD_{67} mRNA and GAT-1 mRNA reported here. A recent *in situ* hybridization study examining the distribution of GAT-1 mRNA and GAD_{67} mRNA in rat brain noted that the regional distribution of hybridization signals was similar but not always coincident, although the distribution of these two mRNAs in the striatum was not reported (Rattray and Priestley, 1994).

Oocytes injected with GAT-1 mRNA display a 100-fold increase in the accumulation of ^{3}H-GABA; a process which is sodium and chloride dependent, saturable (K_m = 7.3 μM) and sensitive to nipecotic acid, a potent GABA uptake inhibitor. Hydropathy plots indicate that GAT-1 protein contains several putative transmembrane domains, consistent with its location in the plasma membrane, and a large extracellular loop (between transmembranes 3 and 4) containing several putative glycosylation sites, a feature of many of the members of the transporter family. Data for a functional role of the GAT-1 GABA trans-

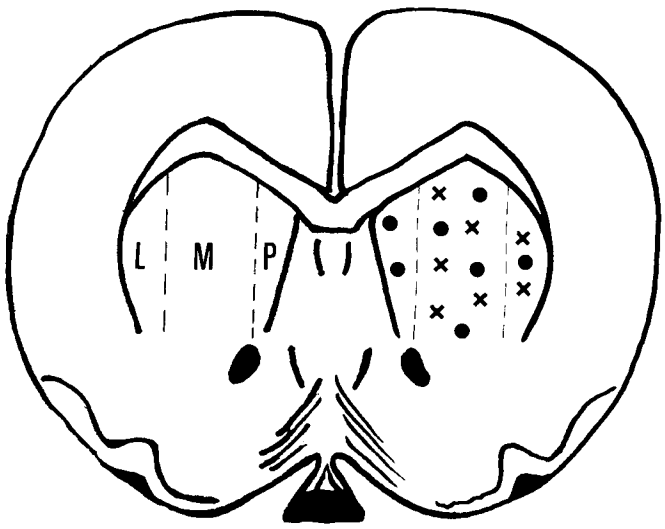

Figure 6. Schematic diagram of a coronal section of rat striatum subdivided into the periventricular (*P*), mid (*M*), and lateral (*L*) regions used in the GAD_{67}-GAT-1 analysis. The regional distribution of cells coexpressing GAT-1 and GAD_{67} mRNAs are indicated by *filled circles* (●) while cells expressing PV and GAD_{67} mRNAs are illustrated by a cross (X). Note that GAT-1/GAD_{67} cells are detected in all three striatal segments (*P, M, and L*), while PV/GAD_{67} cells are detected only in the mid (*M*) and lateral (*L*) segments.

porter *in vivo* is provided by Bolam and colleagues (Bolam et al., 1983), who report that approximately 15% of striatal neurons accumulate ^{3}H-GABA following a local injection. Electron microscopic analysis of these ^{3}H-GABA–accumulating cells suggest that they are of the medium-sized aspiny type, with indented nuclei and a cytoplasm enriched in organelles; morphological features characteristic of local circuit GABA interneurons (Bolam et al., 1985). Further, using this technique of combined autoradiography and electron microscopy, none of the medium-sized spiny neurons examined (presumptive GABAergic projection cells) showed an appreciable accumulation of ^{3}H-GABA. While the chemical phenotype of these GABA-accumulating neurons was not determined directly, Bolam and colleagues comment that these nerve cells are distinguishable from other previously defined striatal cell types including giant neurons and the chemically characterized substance P, enkephalin, and somatostatin cells. Hence, these data are consistent with the hypothesis that GABA-accumulating neurons in the dorsal striatum belong to the GABA/PV and/or GABA/calretinin (Kubota et al., 1993) phenotype.

To determine the neurochemical phenotype of striatal cells enriched in GAT-1 GABA transporter transcripts, we have used here a coexpression technique to visualize simultaneously GAD_{67} and PV gene transcripts in the same tissue section. Light microscopic examination of processed tissue sections in conjunction with computer-assisted image analysis revealed that the vast majority of cells that expressed PV transcripts were selectively enriched in GAD_{67} mRNA (see Figs. 5, 6). These data extend previous immunocytochemical studies that have shown a co-occurrence of GABA and PV immunoreactivity in a small population of cells in the rat (Cowan et al., 1990; Kita et al., 1990; Kubota et al., 1993), monkey, and pigeon (Reiner and Anderson, 1993) striatum. The dual *in situ* hybridization data presented here, thus, provides direct evidence for the synthesis of these two gene transcripts within this discrete population of neurons. In contrast, not all striatal cells enriched in GAD_{67} mRNA expressed PV mRNA; a discrete group of cells was detected, particularly in the periventricular region adjacent to the lateral ventricle, which were enriched in GAD_{67} mRNA alone. These cells had a significantly smaller mean cross-sectional somatic area (approximately 102 μm^2) than high GAD_{67}/PV cells (approximately 152 μm^2) when measured on the same tissue section. These data are in good agreement with the immunocytochemical studies of others (Cowan et al., 1990; Kubota et al., 1993) who report at least two populations of intensely stained GABA-immunoreactive cells, a PV positive group with a cross-sectional range of 150–163 μm^2 and a non-PV population with an average cross-sectional area < 100 μm^2. This diversity in the intensely stained GABA cell population is not always detected however (Kita et al., 1990).

While the chemical phenotype of the non-PV GAD_{67} cells was not determined in this study, it is likely, from their limited number, distribution, and expression of GAD_{67} mRNA, that they belong to another population of GABAergic interneuron that readily accumulates GABA via interaction with the GAT-1 GABA transporter protein. Comparison of cell density, distribution, and size of these non-PV high GAD_{67} cells with the literature suggests that a likely phenotype may be calretinin-immunoreactive cells (Jacobowitz and Winsky, 1991; Bennett and Bolam, 1993), which are also immunopositive for GAD_{67} and GABA in colchicine-treated rats (Kubota et al., 1993). These

Table 1.

Experiment	Oligonucleotide(s)	*N*	Somatic area (μm^2)	Median (μm^2)	Range (μm^2)
A	AP-GAD_{67} = ^{35}S-GAT-1	—	—	—	—
	Periventricular (P)	113	98.27 ± 9.24	97.20	46.28–208.70
	Mid striatum (M)	163	141.08 ± 5.84†	140.40	57.01–279.30
	Lateral striatum (L)	111	166.89 ± 5.61†	166.00	78.48–329.20
B	AP-GAD_{67} = ^{35}S-PV	175	152.40 ± 19.79#	153.61	62.50–345.40
	AP-GAD_{67} ≠ ^{35}S-PV	135	102.48 ± 6.95*	102.57	40.08–194.40
C	^{35}S-PV	136	163.14 ± 64.42	146.95	66.32–382.60

N is the total number of cells sampled on 10 μm thick cryostat sections of dorsal striatum from four rats. For Experiment C cell sizes were determined from two rats. Values are means ± SD.

Not significantly different from value in Experiment C.

* Significantly different from the value for GAD_{67}/PV cells sampled on the same tissue sections ($p < 0.03$, Mann–Whitney *U* test).

† Significantly different from the periventricular region ($p < 0.03$, Mann–Whitney *U* test).

GABA/calretinin-immunoreactive cells are reported to have an average cross-sectional area of 60–90 μm^2 and a range 21.2–178.8 μm^2, slightly smaller than the non-PV high GAD_{67} cells reported here (102.5 μm^2; range 40–194 μm^2). It is possible, however, that the slight differences in cell sizes between the immunocytochemical studies mentioned above and the data reported herein are related to differences in fixation and dehydration of the tissue. Immunocytochemical studies are carried out using dehydrated, perfusion fixed tissue while our measurements were determined from hydrated lightly fixed cryostat sections, where tissue shrinkage will be less extensive. Thus, it is possible that the non-PV GAD_{67}/GAT-1 positive cells reported here correspond to the population of striatal GABA/calretinin-positive cells.

Functional significance for striatal signaling

Striatal PV cells are thought to play a role in modulating the activity of striatal efferents (see Kita, 1993). In contrast to the majority of striatal cells, PV cells are fast spiking with a short-duration action potential and a lower input resistance than other types of striatal interneurons (Kawaguchi, 1993). It is interesting to note, therefore, that this neuronal population is particularly enriched in the 67,000 Mr active form of GAD that is reported to exist saturated with pyridoxal-l-phosphate cofactor (Kaufman et al., 1991) and to be associated with tonically active GABA neurons (Erlander et al., 1991); consistent with the electrophysiological properties of these dorsal striatal PV cells.

PV-immunoreactive axon terminals form synaptic specializations with other PV-immunoreactive cells and the dendrites of medium-sized somata with unindented nuclei (putative striatal efferent cells; Chang and Kita, 1992). Further, it has been shown that PV cells can be activated synchronously, as they are electrically coupled through gap junctions, thus being able to simultaneously inhibit a large number of their target cells. These cells receive a direct excitatory input from the cerebral cortex (Lapper et al., 1992; Kita, 1993) in addition to an indirect thalamic input mediated through local circuit cholinergic cells (Chang and Kita, 1992; Lapper and Bolam, 1992), suggesting that this subpopulation of GABAergic interneurons participate in the feed-forward inhibition of medium-sized spiny efferents (Kita et al., 1990). Further, these cells may play an important role in modulating the activity of striatal efferents in both striatal patch and matrix compartments, as the primary dendrites of PV-immunoreactive cells, in contrast to spiny projection cells, traverse the patch/matrix border and extend into both patch and matrix (Kubota and Kawaguchi, 1993) establishing a chemical connection between these two compartments. Thus, data from this study provides evidence for the expression of GAT-1 protein by PV interneurons if one assumes that GAT-1 transcripts are translated and expressed as functional protein. Thus, the ability of these PV cells to rapidly and effectively reaccumulate GABA released from the presynaptic nerve terminal, through interaction with the GAT-1 GABA uptake protein and, therefore, terminate GABA neurotransmission, may be of physiological significance in reducing the time course of GABAergic feed-forward inhibition enabling further response to cortical inputs.

In summary, this study provides a detailed analysis of the cellular localization of GAT-1 mRNA, a member of the GABA transporter family, in the dorsal striatum of the adult rat. We demonstrate, for the first time, that GAT-1 mRNA is selectively enriched in striatal interneurons that express an abundance of GAD_{67} mRNA, confirming that in the rat dorsal striatum, GAT-1 is a presynaptic marker of GABAergic interneurons including GABA/PV cells. The chemical phenotype of the non-PV GAD_{67}/GAT-1 cells reported herein has yet to be determined.

References

Augood SJ, Emson PC (1994) Adenosine A_{2a} receptor mRNA is expressed by enkephalin cells but not by somatostatin cells in rat striatum: a co-expression study. Mol Brain Res 22:204–210.

Augood SJ, Westmore K, McKenna PJ, Emson PC (1993) Co-expression of dopamine transporter mRNA and tyrosine hydroxylase mRNA in ventral mesencephalic neurons. Mol Brain Res 20:328–334.

Bennett BD, Bolam JP (1993) Characterisation of calretinin-immunoreactive structures in the striatum. Brain Res 609:137–148.

Bolam JP, Clarke DJ, Smith AD, Somogyi P (1983) A type of aspiny neuron in the rat neostriatum accumulates [^{3}H] γ-aminobutyric acid: combination of Golgi-staining, autoradiography, and electron microscopy. J Comp Neurol 213:121–134.

Bolam JP, Powell JF, Wu J-Y, Smith AD (1985) Glutamate decarboxylase-immunoreactive structures in the rat neostriatum: a correlated light and electron microscopic study including a combination of Golgi-impregnation with immunocytochemistry. J Comp Neurol 237:1–20.

Borden LA, Smith KE, Hartig PR, Branchek TA, Weinshank RL (1992) Molecular heterogeneity of the γ-aminobutyric acid (GABA) transport system. J Biol Chem 267:21098–21104.

Braun K, Scheich H, Schachner M, Heizmann CW (1985) Distribution of parvalbumin, cytochrome oxidase activity and ^{14}C-2-deoxyglucose uptake in the brain of the zebra finch. Cell Tissue Res 240:101–115.

Celio MR (1986) Parvalbumin in most γ-aminobutyric acid-containing neurons of the rat cerebral cortex. Science 231:995–997.

Chang HT, Kita H (1992) Interneurons in the rat striatum: relationships between parvalbumin neurons and cholinergic neurons. Brain Res 574:307–311.

Chesselet M-F, Robbins E (1989) Characterisation of striatal neurons expressing high levels of glutamic acid decarboxylase messenger RNA. Brain Res 492:237–244.

Chomczynski P, Sacchi N (1987) Single-step method of RNA isolation by acid guanidinium thiocyanate-phenol-chloroform extraction. Anal Biochem 162:156–159.

Clark JA, Deutch AY, Gallipoli PZ, Amara SG (1992) Functional expression and CNS distribution of a β-alanine-sensitive neuronal GABA transporter. Neuron 9:337–348.

Cowan RL, Wilson CJ, Emson PC, Heizmann CW (1990) Parvalbumin-containing GABA-ergic interneurons in the rat neostriatum. J Comp Neurol 302:197–205.

Epstein P, Means AR, Berchtold MW (1986) Isolation of a rat parvalbumin gene and full length cDNA. J Biol Chem 261:5886–5891.

Erlander MG, Tillakaratne NJK, Feldblum S, Patel N, Tobin AJ (1991) Two genes encode glutamate decarboxylases. Neuron 7:91–100.

Esclapez M, Tillakaratne NJK, Tobin AJ, Houser CR (1993) Comparative localization of mRNAs encoding two forms of glutamic acid decarboxylase with nonradioactive *in situ* hybridization methods. J Comp Neurol 331:339–362.

Esclapez M, Tillakaratne NJK, Tobin AJ, Houser CR (1994) Comparative localization of two forms of glutamic acid decarboxylase and their mRNAs in rat brain supports the concept of functional differences between the forms. J Neurosci 14:1834–1855.

Gerfen CR, Baimbridge KG, Miller JJ (1985) The neostriatal mosaic: compartmental distribution of calcium-binding protein and parvalbumin in the basal ganglia of the rat and monkey. Proc Natl Acad Sci USA 82:8780–8784.

Gomeza J, Giménez C, Zafra F (1994) Cellular distribution and regulation by cAMP of the GABA transporter (GAT-1) mRNA. Mol Brain Res 21:150–156.

Gonzales C, Kaufman DL, Tobin AJ, Chesselet M-F (1991) Distribution of glutamic acid decarboxylase (Mr 67 000) in the basal ganglia of the rat: an immunohistochemical study with a selective cDNA-generated polyclonal antibody. J Neurocytol 20:953–961.

Guastella J, Nelson N, Nelson H, Czyzyk L, Keynan S, Miedel MC, Davidson N, Lester HA, Kanner BI (1990) Cloning and expression of a rat brain GABA transporter. Science 249:1303–1306.

Herbison AE, Augood SJ, McGowan EM (1992) Expression of glu-

tamic acid decarboxylase messenger RNA in rat medial preoptic area neurons during the oestrous cycle and after ovariectomy. Mol Brain Res 14:310–316.

Herrero M-T, Ruberg M, Hirsch EC, Mouatt A, Tobin AJ, Agid Y, Obeso JA, Javoy-Agid F (1993) *In situ* hybridization of GAD mRNA in monkey and human brain: quantification at both regional and cellular levels. Neurosci Lett 157:157–161.

Jablonski E, Molomaw EW, Tulis RH, Ruth JL (1986) Preparation of oligodeoxynucleotide-alkaline phosphatase conjugates and their use as hybridization probes. Nucleic Acids Res 14:6115–6128.

Jacobowitz DM, Winsky L (1991) Immunocytochemical localisation of calretinin in the forebrain of the rat. J Comp Neurol 304:198–218.

Julien J-F, Samama P, Mallet J (1990) Rat brain glutamic acid decarboxylase sequence deduced from a cloned cDNA. J Neurochem 54:703–705.

Kaufman DL, Houser CR, Tobin AJ (1991) Two forms of the γ-aminobutyric acid synthetic enzyme glutamic acid decarboxylase have distinct intraneuronal distributions and co-factor interactions. J Neurochem 56:720–723.

Kawaguchi Y (1993) Physiological, morphological, and histochemical characterization of three classes of interneurons in rat neostriatum. J Neurosci 13:4908–4923.

Kawaguchi Y, Kubota Y (1993) Correlation of physiological subgroupings of nonpyramidal cells with parvalbumin- and calbindin$_{D28K}$-immunoreactive neurons in layer V of the rat frontal cortex. J Neurophysiol 70:387–396.

Kawaguchi Y, Katsumaru H, Kosaka T, Heizmann CW, Hama K (1987) Fast spiking cells in rat hippocampus (CA1 region) contain the calcium-binding protein parvalbumin. Brain Res 416:369–374.

Kita H (1993) GABAergic circuits of the striatum. In: Progress in brain research, Vol 99, Chemical signalling in the basal ganglia (Arbuthnott GW, Emson PC, eds), pp 51–72. New York: Elsevier.

Kita H, Kitai ST (1988) Glutamate decarboxylase immunoreactive neurons in the rat neostriatum: their morphological types and populations. Brain Res 447:346–352.

Kita H, Kosaka T, Heizmann CW (1990) Parvalbumin-immunoreactive neurons in the rat neostriatum: a light and electron microscopic study. Brain Res 536:1–15.

Kubota Y, Kawaguchi Y (1993) Spatial distributions of chemically identified intrinsic neurons in relation to patch and matrix compartments of rat neostriatum. J Comp Neurol 332:499–513.

Kubota Y, Inagaki S, Shimada S, Kito S, Wu J-Y (1987) Glutamate decarboxylase-like immunoreactive neurons in the rat caudate putamen. Brain Res Bull 18:687–697.

Kubota Y, Mikawa S, Kawaguchi Y (1993) Neostriatal GABAergic interneurones contain NOS, calretinin or parvalbumin. Neuroreport 5:205–208.

Lapper SR, Bolam JP (1992) Input from the frontal cortex and the parafascicular nucleus to cholinergic interneurons in the dorsal striatum of the rat. Neuroscience 51:533–545.

Lapper SR, Smith Y, Sadikot AF, Bolam JP (1992) Cortical input to parvalbumin-immunoreactive neurones in the putamen of the squirrel monkey. Brain Res 580:215–224.

Mercugliano M, Soghomonian J-J, Qin Y, Nguyen HQ, Feldblum S, Erlander MG, Tobin AJ, Chesselet M-F (1992) Comparative distribution of messenger RNAs encoding glutamic acid decarboxylases (Mr 65,000 and Mr 67,000) in the basal ganglia of the rat. J Comp Neurol 318:245–254.

Nagai T, McGeer PL, McGeer EG (1983) Distribution of GABA-T-intensive neurons in the rat forebrain and midbrain. J Comp Neurol 218:220–238.

Plogman D, Celio MR (1993) Intracellular concentration of parvalbumin in nerve cells. Brain Res 600:273–279.

Rattray M, Priestley JV (1994) Differential expression of GABA transporter-1 messenger RNA in subpopulations of GABA neurones. Neurosci Lett 156:163–166.

Reiner A, Anderson KD (1993) Co-occurrence of γ-aminobutyric acid, parvalbumin and the neurotensin-related neuropeptide LANT6 in pallidal, nigral and striatal neurons in pigeons and monkeys. Brain Res 624:317–325.

Schwartz LM, Kay BK (1988) Differential expression of the Ca^{2+}-binding protein parvalbumin during myogenesis in *Xenopus laevis*. Dev Biol 128:441–452.

Seto-Ohshima A, Emson PC, Berchtold MW, Heizmann CW (1989) Localisation of parvalbumin mRNA in rat brain by *in situ* hybridisation histochemistry. Exp Brain Res 75:653–658.

Vincent SR, Johansson O (1983) Striatal neurones containing both somatostatin- and avian pancreatic polypeptide (APP)-like immunoreactivities and NADPH-diaphorase activity: a light and electron microscopic study. J Comp Neurol 217:264–270.

Xia Y, Poosch MS, Whitty CJ, Kapatos G, Bannon MJ (1993) GABA transporter mRNA: *in vitro* expression and quantitation in neonatal rat and postmortem human brain. Neurochem Int 22:263–270.